J. Opt. B: Quantum Semiclass. Opt. **2** (2000) 413–420. Printed in the UK PII: S1464-4266(00)09621-X

Stabilization of feedback-induced instabilities in semiconductor lasers

T Heil, I Fischer and W Elsäßer

Institute of Applied Physics, Darmstadt University of Technology, Schloßgartenstraße 7, 64289 Darmstadt, Germany

Received 17 November 1999, in final form 1 March 2000

Abstract. We present extensive studies on feedback-induced instabilities in semiconductor lasers (SLs) subject to delayed optical feedback. We demonstrate that a sufficient reduction of the linewidth enhancement factor α changes the dynamical structure of the system such that permanent emission in a stable emission state is achieved. This behaviour can be well understood on the basis of the Lang–Kobayashi rate equation model. We give first experimental evidence for its major theoretical predictions concerning the stable emission state and investigate the robustness of this stable state against external perturbations. We demonstrate that noise-induced escape from the basin of attraction of the stable state shows similarities to the classical problem of thermally induced escape from a potential well. Thus, we have developed and realized experimentally an efficient concept to avoid and stabilize feedback-induced instabilities in SLs.

Keywords: Semiconductor lasers, nonlinear dynamics

1. Introduction

Semiconductor lasers (SLs) subject to delayed optical feedback, e.g. from the facets of an optical fibre, an optical disc or an external mirror, exhibit a variety of complex dynamical phenomena. In practical applications, these feedback-induced instabilities may severely degrade the performance of the lasers. Therefore, a profound understanding of the dynamical phenomena in SLs is indispensable in order to avoid, or even to utilize, the instabilities in future applications. This necessary understanding of the dynamics of the system has been boosted recently by using the methods of nonlinear dynamics. From the nonlinear dynamics point of view, SLs with optical feedback are considered as a model system for investigations of delay systems in general. Delay systems often show complex dynamical behaviour due to the infinite number of possible degrees of freedom available to these systems. A further peculiarity of SLs with delayed optical feedback is the extraordinary strong amplitude–phase coupling of the optical field in the SL, which is described by the linewidth enhancement factor α. This strong nonlinearity in combination with the delayed feedback gives rise to the complex dynamical behaviour investigated in this paper.

The main concern of the present work is to investigate the influence of the amplitude–phase-coupling nonlinearity α on the dynamics of the system. In particular, we aim to avoid the feedback-induced instabilities. Therefore, we present extensive experimental investigations of the dynamical behaviour of SLs subject to delayed optical feedback in dependence on three parameters most relevant for the dynamics of the system: the injection current I, the feedback rate γ and the linewidth enhancement factor α. We demonstrate that for a very low value of $\alpha \approx 1$ the system continuously emits on a stable emission state. This behaviour has been predicted by the Lang–Kobayashi (LK) rate equation model. We show that the stable emission state indeed is the single external-cavity high-gain mode (HGM) predicted by the LK model by giving first experimental evidence for three major predictions of the LK model concerning the HGM. Finally, we investigate the robustness of the HGM against external perturbations by superimposing white electronic noise onto the injection current of the laser. In particular, we study the noise-induced escape from the HGM in terms of a first-passage-time problem and compare our results to the Henry–Kazarinov (HK) model. In addition, we demonstrate that the noise-induced escape from the basin of attraction of the HGM shows similarities to the classical problem of thermally induced escape from a potential.

In the following section, we characterize the dynamics of SLs subject to delayed optical feedback and summarize some of the proposed theoretical explanations. In particular, we will focus on the LK rate equation model, which predicts the existence of the HGM, and its coexistence with the complex dynamics. Finally, we discuss possibilities to stabilize the laser emission on the HGM.

2. Coexistence of complex dynamics and stable emission

According to the phenomenological classification by Tkach and Chraplyvy [1], feedback-induced instabilities in SLs occur over the wide range of feedback levels between -45 dB and -10 dB. Since these instabilities are

1464-4266/00/030413+08$30.00

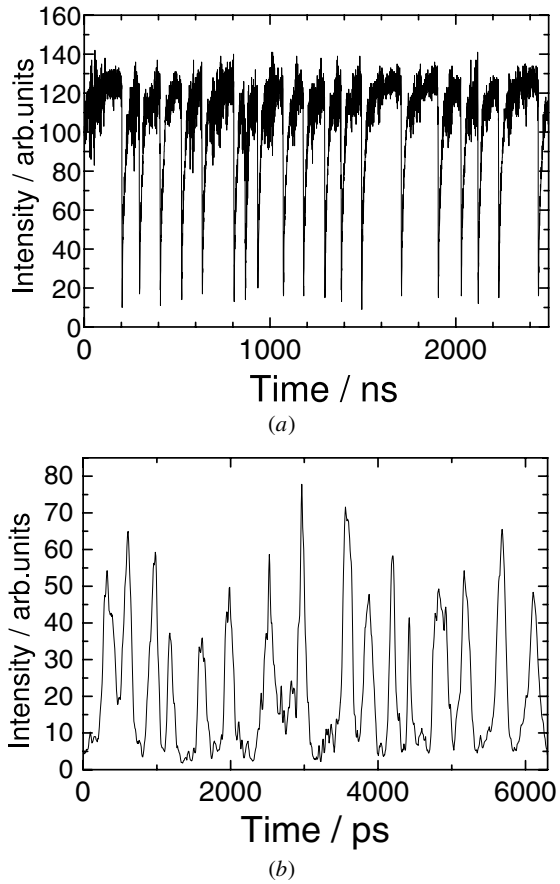

Figure 1. Intensity time series recorded for $I = 1.05 I_{\mathrm{th,sol}}$ and $\gamma = 25\ \mathrm{ns}^{-1}$. (*a*) Oscilloscope single-shot measurement, bandwidth 1 GHz. (*b*) Streak camera single-shot measurement, bandwidth more than 50 GHz.

associated with a drastic increase of the spectral linewidth of the SL, this dynamical regime is referred to as coherence collapse [2]. In this regime, the intensity dynamics are characterized by a wide range of timescales [3]. Figure 1 shows a typical example recorded for injection currents close to the solitary laser threshold. Figure 1(*a*) depicts irregular fluctuations of the laser intensity on a timescale of microseconds, which is very slow compared with the relaxation oscillation frequency of the SL as a typical semiconductor internal frequency. However, figure 1(*b*) depicting the same dynamics on faster timescales shows that indeed there is a fast pulsating behaviour underlying these slow dynamics. Because of these different timescales, theoretical and experimental investigations of this system are challenging and a variety of different models describing these feedback-induced instabilities have been proposed. A key point in this discussion has been the relative importance of determinism and noise governed mechanisms, and the interplay of the two in the dynamics [4–8]. Furthermore, the role of the number of optical modes [9–12] involved in the laser emission, and effects of asymmetry [13–15], have been intensively discussed.

In this paper, we focus on the LK rate equation model [16] because this model, despite its simplifications, successfully explains our experimental results. The LK equations for the complex electrical field E and the carrier number $n(t) = N(t) - N_0$ with respect to the solitary level N_0 are

$$\dot{E}(t) = \tfrac{1}{2}(1 + \mathrm{i}\alpha)\xi n(t)E(t) + \gamma E(t-\tau)\mathrm{e}^{-\mathrm{i}\omega_0\tau} \qquad (1)$$

$$\dot{n}(t) = (p-1)\frac{I_{\mathrm{th}}}{e} - \frac{n(t)}{T_1} - (\Gamma_0 + \xi n(t))P(t). \qquad (2)$$

The optical feedback is taken into account by γ and the delay time τ. The electrical field is normalized so that $P(t) = |E(t)|^2$ is the photon number; ω_0 represents the optical frequency of the solitary laser, ξ the differential gain, Γ_0 the cavity decay rate, T_1 the carrier lifetime, I_{th} the bias current at solitary laser threshold, e the electron charge and p the pump parameter. α accounts for the carrier-induced variation of real and imaginary parts of the semiconductor material's susceptibility $\chi(n) = \chi_r(n) + \mathrm{i}\chi_i(n)$. α is defined as follows [19, 20]:

$$\alpha = -\frac{\mathrm{d}(\chi_r(n))/\mathrm{d}n}{\mathrm{d}(\chi_i(n))/\mathrm{d}n}. \qquad (3)$$

We begin our analysis by reviewing some properties of the LK model. First, we consider the fixed points and their stability properties. Each fixed point of the LK equations corresponds to a constant optical frequency $\omega_0 + \Delta\omega$ and a constant carrier number n [5]. The location of these fixed points in frequency-inversion space is given by the following equations:

$$\Delta\omega\tau = \gamma\tau\sqrt{1+\alpha^2}\sin\{(\omega_0 + \Delta\omega)\tau + \arctan\alpha\} \qquad (4)$$

$$(\gamma\tau)^2 = \left(\Delta\omega\tau - \alpha\frac{\tau\xi n}{2}\right)^2 + \left(\frac{\tau\xi n}{2}\right)^2. \qquad (5)$$

As can be seen from equations (4) and (5), the fixed points form an ellipse around the solitary laser mode in frequency-inversion space. The eccentricity of this ellipse is determined by the value of α. Decreasing α reduces the eccentricity of the ellipse, i.e. for $\alpha = 0$, the fixed points of the system are located on a circle around the solitary laser mode. Three types of fixed point are present in the system [6]: first, fixed points called antimodes exhibiting a saddle-node instability which physically correspond to destructive interference between the laser cavity and the external cavity; second, fixed points called modes corresponding to constructive interference, which are destabilized via Hopf bifurcation; third, located at the very low-frequency, high-gain end of the ellipse, the so-called maximum-gain mode [17], which always remains stable. In addition, all modes in the vicinity of the maximum-gain mode which satisfy

$$-\arctan(1/\alpha) < (\omega_0 + \Delta\omega)\tau < 0 \qquad (6)$$

also remain stable. Thus, the number of these stable HGMs increases with decreasing α. This structure of the LK equation gives rise to two different dynamical states. On the one hand, the trajectory may move irregularly on the system of destabilized fixed points. On the other hand, the trajectory may stay on the HGM.

The LK model explains the complex dynamics of SLs with optical feedback as a consequence of an irregular movement of the trajectory on the system of destabilized

fixed points described above [3]. These complex dynamics are characterized by a broad power spectrum. Emission on the HGM, however, is a different dynamical state and not part of this complex dynamics. The complex dynamics often appears to be the only existing dynamical state because in these cases the basin of attraction of the HGM is extremely small. Nevertheless, for certain parameter regions, coexistence of the stable HGM with the complex dynamical behaviour has been demonstrated in recent experimental investigations [18].

In the present contribution, we aim to stabilize the laser emission on the HGM and, thus, to avoid the occurrence of the feedback-induced instabilities in principle. Our concept is to reduce the strong amplitude–phase coupling of the optical field described by α. Theoretically, the effect of a reduction of this main nonlinearity of the system is threefold. First, according to equation (5), the eccentricity of the ellipse of fixed points decreases with decreasing α, i.e. the distance between stable and unstable fixed points increases [6]. Second, from equation (4) it results that the total number of fixed points decreases with decreasing α, whereas, according to equation (6), the number of stable modes increases [17]. Third, the size of the local attractors of each destabilized mode decreases [21]. Therefore, according to the LK model, decreasing α leads to an enlarging basin of attraction of the HGM, and an increasing stability of the HGM. In the following section, we present extensive experimental investigations of the influence of a reduction of α on the dynamics of the system.

3. The influence of a reduction of α on the dynamics of SLs with feedback

In this section, we first describe the experimental method with which we control the value of α. Then, we present experimental investigations of the dynamics of the system in dependence on three parameters most relevant for the dynamics of the system, i.e. γ, I and α. We will demonstrate a conspicuous stabilization of the laser emission on HGM with decreasing α over large parameter regimes.

3.1. Controlling α

In order to control the value of α, we take advantage of the strong spectral dependence of α. Experimental and theoretical results have demonstrated that α decreases continuously with decreasing wavelength [22–25]. This effect is mainly due to the strongly increasing differential gain because the changes of the refractive index with the carrier density vary only slightly. Consequently, we control α by shifting the emission wavelength of the system away from the gain maximum of the solitary laser. We achieve this by placing an etalon inside the external cavity. Tilting the etalon allows us to shift the overall gain profile of the system, which can be described as the superposition of the gain curve of the solitary laser, the Airy transmission function of the etalon and the effective reflectivity of microscope objective (MO) and feedback mirror. Thus, we tune the emission wavelength of the system without changing the gain profile of the SL. This particular wavelength shift allows us to control the value of α. In our discussion, we neglect the slight changes of the material gain profile due to the wavelength shift, because the resulting effects are small compared with the changes of α.

Figure 2 depicts a scheme of the experimental setup. The laser is a bulk Fabry–Pérot laser diode (Hitachi HLP1400), which is driven by an ultra-low-noise constant-current source and temperature stabilized to better than 0.01 K. The laser beam is collimated by an anti-reflection coated MO. The feedback branch consists of a high-reflection mirror, and a neutral-density filter. The delay time of the external cavity amounts to 3.3 ns. A key element is the intracavity etalon with a transmission bandwidth of approximately 2.1 THz. Due to the spectral selectivity of the etalon, the SL emission is dominated by one longitudinal diode mode. However, it does not suppress the corresponding external cavity modes due to its large transmission bandwidth [26]. The etalon allows us to tune the emission wavelength of the laser over a range of about 10 nm around the solitary gain maximum. The intensity dynamics is detected by a single-shot streak camera with an analogue bandwidth of more than 50 GHz and by a fast avalanche photodiode (APD) with greater than 3 GHz bandwidth. The power spectrum of the APD signal is recorded by an electrical spectrum analyser. The corresponding time series are low-pass filtered with the cut-off frequency at 1 GHz and detected by a fast oscilloscope of the same bandwidth. The time averaged intensity is measured by a p–i–n photodiode. The optical spectrum is analysed via a grating spectrometer with a resolution of 0.1 nm in order to resolve the longitudinal diode modes and to monitor the absolute emission wavelength of the laser. In addition, a confocal scanning Fabry–Pérot interferometer is used to resolve the external cavity modes. The free spectral range of the interferometer amounts to 2 GHz, the resolution to 10 MHz. An optical isolator shields the laser from unwanted external feedback from the detection branch.

In order to obtain maximum information about the effect of a variation of α on the dynamics of the system, we choose the following experimental method. First, we adjust the emission wavelength of the system and, thus, select the desired value of α. Then, we adjust the feedback rate γ using the neutral-density filter. Finally, we vary the injection current over the whole accessible range and record the resulting dynamical behaviour. Repeating this procedure for different values of γ, we obtain a γ–I-space diagram providing both detailed information and a global view over dynamics of the system for the selected value of α. In the following section, we identify the effects of a changing α on the dynamics of the system by comparing γ–I-space diagrams recorded for different values of α.

3.2. Decreasing α stabilizes the system on HGM

Figure 3 depicts three γ–I-space diagrams recorded for three different emission wavelengths, i.e. 841, 838.2 and 835.5 nm. The values of α corresponding to these wavelengths have been determined using the method of Henning and Collins [27], which is based on measurements of the Fabry–Pérot resonances in the spontaneous emission spectrum of the laser [28]. We obtain $\alpha = 2.8 \pm 0.5$ at

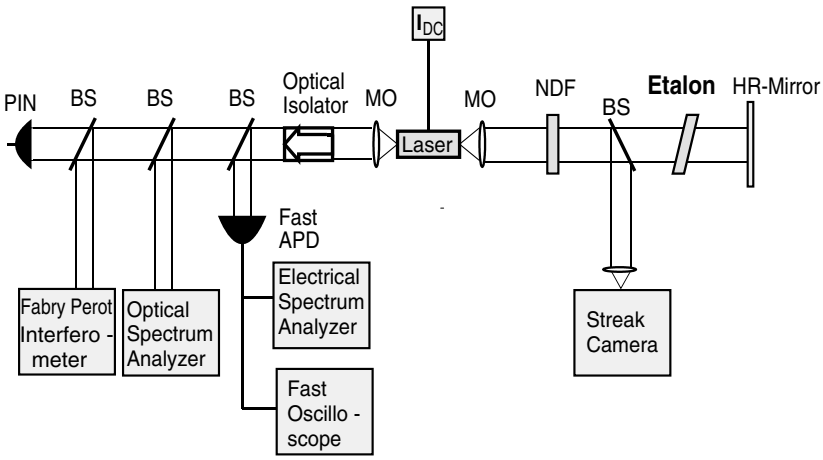

Figure 2. Experimental setup allowing us to control the value of α and detect the temporal and spectral dynamics.

841 nm, $\alpha = 2.1 \pm 0.4$ at 838.2 nm and $\alpha = 1.6 \pm 0.3$ at 835.5 nm. These values are in good agreement with previous results for this type of laser [22, 23].

All γ–I-space diagrams depicted in figure 3 exhibit similar features: the threshold reduction due to the optical feedback and two main dynamical regimes, i.e. the regime of coexistence of stable emission on the HGM with complex dynamics, and the regime of complex dynamics. A more detailed characterization of these regimes can be found in [29].

Only within the coexistence regime does the trajectory have a finite probability to reach the HGM. Once the trajectory has reached the dynamically stable HGM, it can nevertheless be ejected again by external or internal perturbations because the HGM is not yet sufficiently stable. Since we aim to stabilize the laser emission on the HGM, we focus our discussion on this coexistence regime. Figure 3 demonstrates that the coexistence regime drastically increases for decreasing α. Furthermore, the average times of stable emission on the HGM increase strongly with decreasing α. For $\alpha = 1.6$ residence times on the HGM exceeding 1 min are observed for considerable parameter regions in γ–I space, preferably on the stronger-feedback side of the coexistence regime.

The comparison of the three γ–I-space diagrams depicted in figure 3 leads to the following results:

(i) The HGM becomes more stable for decreasing α. Consequently, the emission on the HGM becomes more robust against internal or external noise.
(ii) The HGM can be reached more easily for drastically increasing parameter regimes for decreasing α. This is consistent with an enlarging basin of attraction of the HGM which is predicted by theory.

These results strongly indicate that the laser emission can indeed be stabilized by a reduction of α. However, the combination of etalon and SLs used in our setup above does not permit us to further decrease this value because of the limited transmission bandwidth of the etalon and the decreasing gain of the SL. Consequently, we alternatively approach the task of further reducing α by selecting multi-quantum-well distributed-feedback (MQW-DFB) lasers for our investigations.

Quantum-well (QW) lasers are known to have a considerably lower α than bulk lasers such as the HLP1400. This is mainly due to the dominant increase of the differential gain in QW lasers [22, 23]. Furthermore, DFB lasers have the great advantage that their emission wavelength is determined by the Bragg grating. Thus, the emission wavelength can be tuned technologically to higher energies independently of the gain profile of the semiconductor material. Thus, α can be selected by design in DFB lasers [24]. An additional small continuous variation of α is possible by temperature tuning the material gain curve relative to the lasing frequency selected by the DFB grating.

In the next section, we experimentally investigate the consequences of a further reduction of α for the dynamics of the system by using an MQW-DFB laser with a very low value of α.

4. Experiments using a low-α MQW-DFB laser

In this section, we first describe our new complimentary experimental setup. Then, we present detailed experimental investigations of the properties of the HGM. Finally, we investigate the robustness of the HGM against external perturbations.

4.1. Laser structure and experimental setup

Figure 4 shows the experimental setup. The laser is an MQW-DFB laser emitting at 1.55 μm produced by Alcatel SEL. The laser facet heading towards the external cavity is anti-reflection coated. However, the κL of the DFB grating of the laser [30] is 0.7, corresponding to reflectivities similar to those of the cleaved facets of the HLP1400. External electronic noise can be added to the injection current via the Bias Tee. The electronic noise is Gaussian with a bandwidth of 1.1 GHz. The fast photodiode has a bandwidth of 750 MHz. The delay time τ of the external cavity is 4 ns. The specifications of the other elements of the setup are similar to those described in section 3.

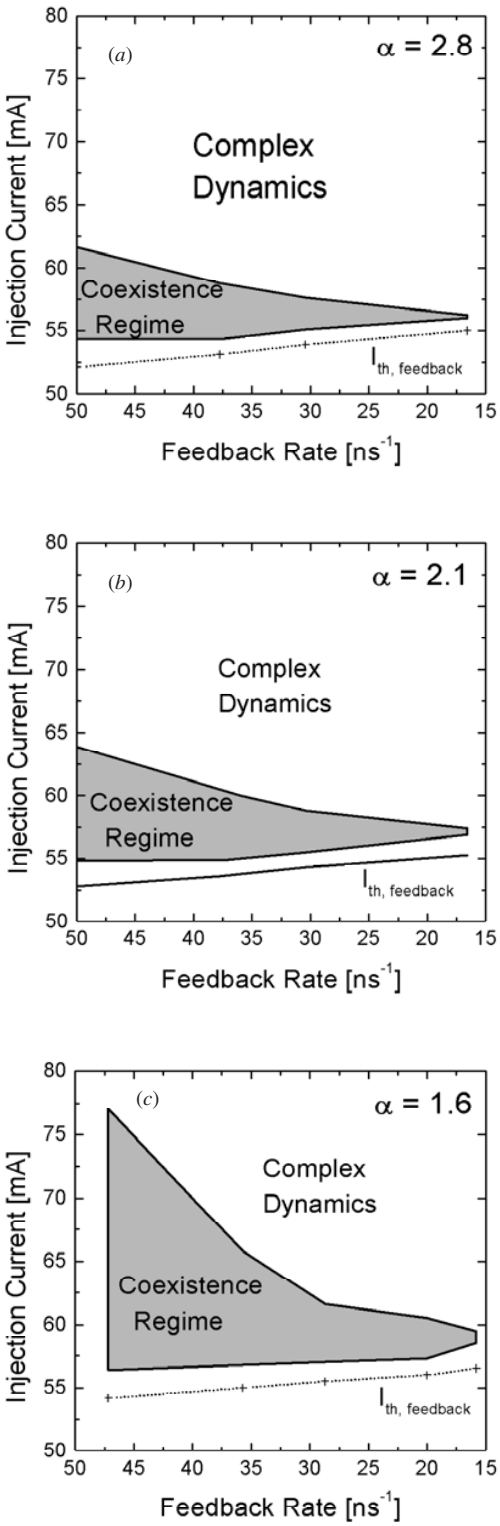

Figure 3. The dynamical behaviour of SLs with optical feedback in dependence on the injection current I and the optical feedback strength γ for: (*a*) 841 nm corresponding to $\alpha = 2.8 \pm 0.5$, (*b*) 838.2 nm corresponding to $\alpha = 2.1 \pm 0.4$, (*c*) 841 nm corresponding to $\alpha = 1.6 \pm 0.3$.

4.2. Stable emission for low-α laser

We have measured the value of α of the MQW-DFB laser to be 0.95 ± 0.2. Consequently, we are close to a critical

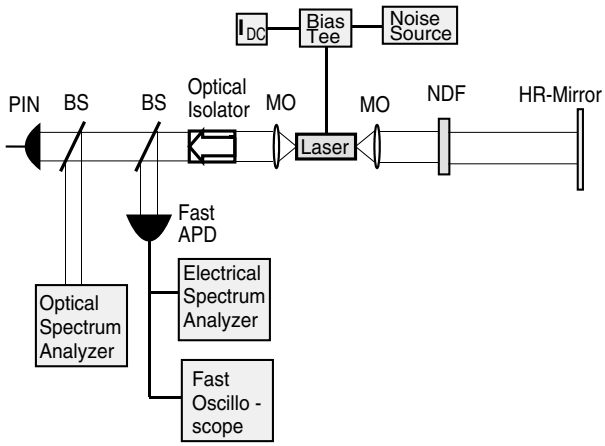

Figure 4. The experimental setup using the MQW-DFB laser allowing noise-induced escape studies.

value of α below which certain feedback-induced instabilities may disappear. Depending on many other parameters, this value typically is $\alpha \leqslant 1$ [31]. In order to obtain an overview on the dynamics of the system for this very low α, we record another γ–I-space diagram. We find that for the entire parameter range covered by the diagrams shown in figure 3, the laser emission is always stable: for these intermediate feedback levels, the laser emission remains stable for injection currents exceeding twice the solitary laser threshold. For even higher injection currents, the system shows the complex dynamics which is also observed in other SLs for this parameter region. The higher the feedback level γ, the higher the injection current for which the transition to the complex dynamics occurs. The extension of the stable emission regime in γ–I space resembles regime V depicted in [32]. The extraordinary stability of the stable emission state allows detailed investigations of its properties, which are presented in the following section.

4.3. The stable emission state is indeed the HGM

The stability analysis of the fixed points of the LK equations leads to the following predictions concerning the HGM. First, the frequency of the HGM is shifted relative to the solitary laser mode to lower frequencies, i.e. larger wavelengths [17]. The amount of the frequency shift is given by

$$\Delta\omega\tau = \alpha\gamma\tau. \tag{7}$$

Furthermore, according to equation (7), the frequency shift should linearly depend on the feedback rate γ and the slope of this linear dependence is given by α. Finally, the linewidth of the HGM, $\delta\lambda_{\mathrm{HGM}}$, should decrease relative to the linewidth of the solitary laser $\delta\lambda_{\mathrm{SOL}}$ [33]:

$$\delta\lambda_{\mathrm{HGM}} = \delta\lambda_{\mathrm{SOL}}/(1+\gamma\tau)^2. \tag{8}$$

The extraordinary stability of the stable emission state over wide parameter ranges allows us for the first time to check these theoretical predictions by analysing the optical spectra of the system. Figure 5 shows the optical spectra of the solitary laser, and the laser with feedback in the stable emission state. In agreement with theory, the laser line with

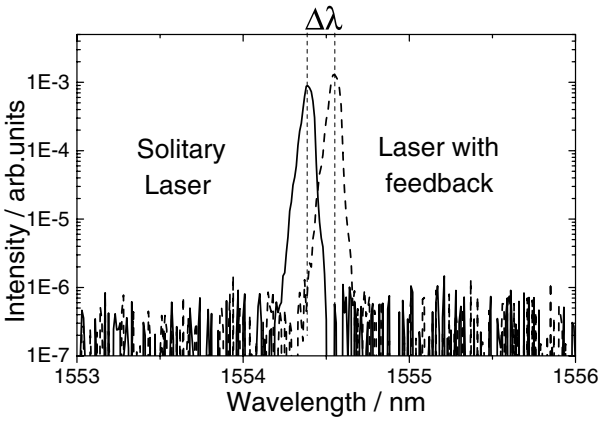

Figure 5. Optical spectra of the MQW-DFB laser: solid curve, stable emission without optical feedback; dotted curve, stable emission with optical feedback.

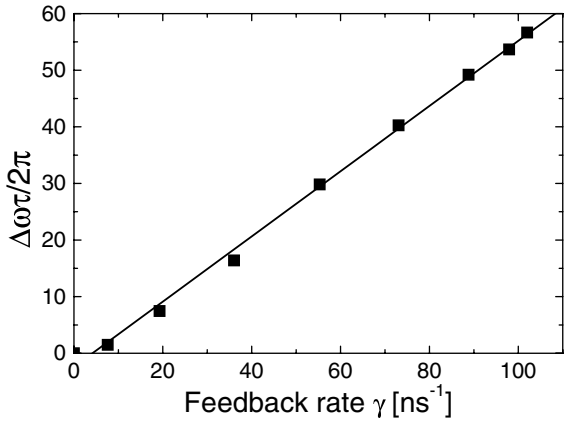

Figure 6. Frequency shift of the stable emission state with feedback relative to the solitary laser in dependence on the feedback level (solid squares). The solid line shows a linear fit.

feedback is shifted to longer wavelength. In order to check the second prediction concerning the HGM, we repeat this measurement for different values of the feedback rate γ. Figure 6 shows that the frequency shift indeed is linearly dependent on γ. This linear dependence remains unchanged under variation of the injection current. Finally, according to equation (7), the slope of this line should be given by the value of α. From the linear fit presented in figure 6, we find a value of $\alpha = 1.1$. This value is in very good agreement with the value we have obtained using the method of Henning and Collins. So, the experimental results presented in this section confirm three major predictions of the LK model concerning the HGM, i.e. frequency shift, dependence on γ and dependence on α. Therefore, we conclude that the stable emission state is indeed the HGM.

The very good agreement of experiment and theory underlines the importance of equation (8) describing the scaling of the spectral linewidth of the HGM with $\gamma\tau$. In the present experiment $\gamma\tau$ is as large as 300. This value should result in a linewidth narrowing by almost five orders of magnitude. Since the solitary laser linewidth typically is of the order of some tens of MHz, linewidths in the sub-kHz range should be easily accessible. In our experimental setup, we are not able to observe this effect because even the solitary laser linewidth cannot be resolved with the grating spectrometer. However, for the HLP1400, we observe a linewidth narrowing of more than one order of magnitude in the Fabry–Pérot interferometer spectrum, again limited by the resolution of 10 MHz of the interferometer. To sum up, emission on the HGM might have applications in spectroscopy as a stable, tunable, and very narrow-linewidth light source. For these applications, in which feedback-induced instabilities need to be avoided, the robustness of the HGM against external perturbations is essential. Therefore, we present systematic investigations of this point in the next section.

5. Noise-induced escape from the basin of attraction of the HGM

In order to test the stability of the HGM against external perturbations, we add variable amounts of white electronic noise to the injection current of the laser. In the following, we investigate parameter regimes for which the system without external noise or perturbations always emits on the HGM. Increasing the noise from very low levels, we observe the existence of a certain threshold noise level below which the trajectory of the system remains on the HGM. Increasing the external noise level above this threshold level, the trajectory can be ejected from the HGM. Consequently, the system jumps back and forth between the HGM and complex dynamics. Increasing the noise level even further, the system finally no longer reaches the HGM, and the complex dynamics prevail. The power spectrum of the complex dynamics is similar to the power spectrum of other laser types which are unstable under similar conditions without external noise. Thus, we conclude that, even though the HGM is very stable, the system of unstable fixed points persists, and that the observed complex dynamics takes place on this unstable fixed point system.

5.1. A first-passage-time problem

In order to investigate the phase space of the system around the HGM, we concentrate on intermediate noise levels for which the system alternates between stable emission and complex dynamics. We find that the system jumps back and forth between these two states on extremely slow timescales on the order of milliseconds. Figure 7 shows experimental distribution functions (DFs) of the escape times from the HGM for two different noise levels. In both cases, the DFs show an exponential decay. This exponential decay is observed for all noise levels, and indicates that a stochastic process governs the underlying mechanism. In particular, within the statistical error bars, all DFs exhibit the following characteristic dependence on the average escape time $\langle\tau\rangle$:

$$\xi(t) \propto \mathrm{e}^{-\frac{t}{\langle\tau\rangle}}. \tag{9}$$

The same formula has been obtained theoretically by Sukow *et al* [34] from an extension of the HK model [8]. Originally, the HK model was designed to explain the low-frequency fluctuation (LFF) phenomenon in terms of a first-passage-time problem: an SL with optical feedback is prepared in its stable state, for which a potential is assumed; the HK

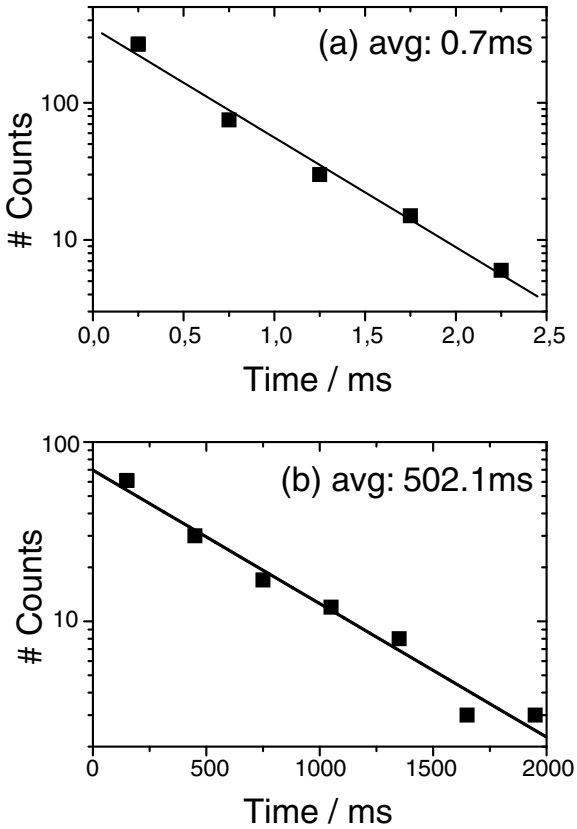

Figure 7. DFs of the escape times from the HGM for two different noise levels, (*a*) −56 dB m MHz^{-1} and (*b*) −58 dB m MHz^{-1} (solid squares). The solid lines depict linear fits.

model studies spontaneous emission noise-induced escapes from this potential. Interestingly, the HK model fails to describe the DFs for the LFF case [34], but agrees well with our experimental results. In addition, the HK model predicts the following approximation for the potential depth U, i.e. the stability of the stable state:

$$U \propto \frac{\gamma^4}{\alpha^4 I^2}. \tag{10}$$

This prediction is consistent with our experimental results. The stability of the HGM increases with decreasing α, increases with increasing feedback strength γ and decreases with increasing injection current I.

5.2. Similarity to thermally induced escape from a potential

As demonstrated by figure 7, the average escape times $\langle\tau\rangle$ depend very sensitively on the noise level R. We have systematically investigated this sensitive dependence. Figure 8 shows the average escape times plotted versus the inverse noise level. Over several decades, $\langle\tau\rangle$ increases exponentially with the inverse noise level:

$$\log\langle\tau\rangle \propto \frac{1}{R}. \tag{11}$$

It is interesting to note that this characteristic dependence exhibits similarity to the classical problem of thermally

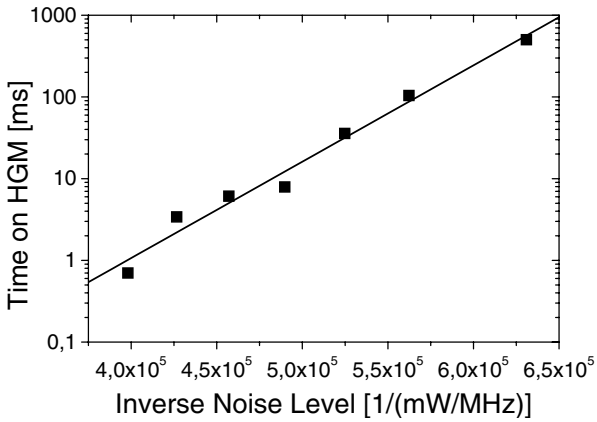

Figure 8. Average escape times from the HGM in dependence on the inverse noise level (solid squares). The solid line depicts a linear fit.

induced escape from a potential well. In this problem, the temperature dependence of the average escape time $\langle\tau\rangle$ is given by the well known, phenomenological Arrhenius factor [35, 36]:

$$\log\langle\tau\rangle \propto \frac{E_A}{k_B T}. \tag{12}$$

E_A is the activation energy of the potential, and k_B is Boltzmann's constant. So, the average escape time in this problem increases exponentially with the inverse temperature T. These first experimental results encourage further experimental investigations to determine the mechanism underlying this characteristic behaviour.

6. Conclusions

We have presented an efficient concept to avoid and control feedback-induced instabilities in SLs subject to delayed optical feedback. This concept uses theoretical predictions of the LK rate equation model. According to this model, the dynamical structure of the system consists of two separate states: a set of destabilized fixed points responsible for the instabilities, and the stable HGM. The complex dynamics which takes place on the system of destabilized fixed points often prevails since the basin of attraction of the HGM is very small. The concept presented in this paper exploits the fact that the HGM nevertheless is accessible within a certain parameter regime, in which the HGM coexists with the complex dynamics. The aim is to stabilize the laser emission on the HGM and thereby suppress the instabilities. In a first step, we have demonstrated that the HGM becomes more stable and more easily accessible for a decreasing linewidth enhancement factor α. Thus, we have confirmed the importance of α as a key parameter for the dynamics of the system. In a second step, we have demonstrated that a sufficient reduction of α changes the dynamical structure of the system so that permanent emission on the HGM is achieved. For $\alpha \approx 1$, we have observed robust stable emission over very large parameter regimes. Detailed investigations of this stable emission state have confirmed central predictions of the LK model concerning the HGM, which confirm that the stable emission state indeed is the

HGM. In order to investigate the stability properties of the HGM, we have added white electronic noise to the injection current. We have demonstrated that the noise-induced escape process away from the HGM can be described as a first-passage-time problem. In particular, the predictions of the HK model concerning the DFs and the potential depth are consistent with our experimental results. Finally, we have demonstrated that the noise-induced escape from the basin of attraction of the HGM exhibits similarity to the classical problem of thermally induced escape from a potential well.

We conclude that the performance of SLs in practical applications can be substantially improved by a sufficient reduction of α. Low-α lasers exhibit two most desirable properties for practical applications: insensitivity to delayed optical feedback and chirpless operation. Values of $\alpha \approx 0$ seem to be feasible in, preferably modulation doped, QW–DFB lasers with a Bragg grating detuned to shorter wavelengths. Furthermore, stable emission on the HGM may find applications in spectroscopy and other fields as a simple, narrow-linewidth, tunable light source.

References

[1] Tkach R W and Chraplyvy A R 1986 *J. Lightwave Technol.* **4** 1665
[2] Lenstra D, Verbeek B H and den Boef A J 1985 *IEEE Trans. Quantum Electron.* **21** 674
[3] Fischer I, van Tartwijk G H M, Levine A M, Elsäßer W, Göbel E O and Lenstra D 1996 *Phys. Rev. Lett.* **76** 220
[4] Mørk J, Tromborg B and Christiansen P L 1988 *IEEE Trans. Quantum Electron.* **24** 123
[5] Sano T 1994 *Phys. Rev.* A **50** 2719
[6] van Tartwijk G H M, Levine A M and Lenstra D 1995 *IEEE Select. Top. Quantum Electron.* **1** 466
[7] Hohl A, van der Linden H J C and Roy R 1995 *Opt. Lett.* **20** 2396
[8] Henry C H and Kazarinov R F 1986 *IEEE Trans. Quantum Electron.* **22** 294
[9] Huyet G, Balle S, Giudici M, Giacomelli G and Tredicce J R 1998 *Opt. Commun.* **149** 341
[10] Heil T, Mulet J, Fischer I, Elsäßer W and Mirasso C R 1999 *Opt. Lett.* **24** 1275
[11] Vashenko G, Giudici M, Rocca J J, Menoni C S, Tredicce J R and Balle S 1998 *Phys. Rev. Lett.* **81** 5536
[12] Sukow D W, Heil T, Fischer I, Gavrielides A, Hohl-AbiChedid A and Elsäßer W 1999 *Phys. Rev.* A **60** 667
[13] Besnard P, Meziane B and Stephan G 1993 *IEEE Trans. Quantum Electron.* **29** 1271
[14] de Tomasi F, Cerboneschi E and Arimondo E 1994 *IEEE Trans. Quantum Electron.* **30** 2277
[15] Sacher J, Elsäßer W and Göbel E O 1991 *IEEE Trans. Quantum Electron.* **27** 373
[16] Lang R and Kobayashi K 1980 *IEEE Trans. Quantum Electron.* **16** 347
[17] Levine A M, van Tartwijk G H M, Lenstra D and Erneux T 1995 *Phys. Rev.* A **52** R3436
[18] Heil T, Fischer I and Elsäßer W 1998 *Phys. Rev.* A **58** R2672
[19] Haug H and Haken H 1967 *Z. Phys.* **204** 262
[20] Henry C H 1982 *IEEE Trans. Quantum Electron.* **18** 259
[21] Masoller C and Abraham N B 1998 *Phys. Rev.* A **57** 1313
[22] Osinski M and Buus J 1987 *IEEE Trans. Quantum Electron.* **23** 9
[23] Hofmann M, Koch M, Heinrich H J, Weiser G, Feldmann J, Elsäßer W, Göbel E O, Chow W W and Koch S W 1994 *IEE Proc. Optoelectron.* **141** 127
[24] Yamanaka T, Yoshikuni Y, Lui W, Yokoyama K and Seki S 1992 *IEEE Photon. Technol. Lett.* **4** 1318
[25] Vahala K, Chiu L C, Margalit S and Yariv A 1983 *Appl. Phys. Lett.* **42** 631
[26] Yousefi M and Lenstra D 1999 *IEEE Trans. Quantum Electron.* **35** 970
[27] Henning I D and Collins J V 1983 *Electron. Lett.* **19** 927
[28] Hakki B W and Paoli T L 1975 *J. Appl. Phys.* **46** 1299
[29] Heil T, Fischer I and Elsäßer W 1999 *Phys. Rev.* A **60** 634
[30] Agrawal G P and Dutta N K 1986 *Long Wavelength Semiconductor Lasers* (New York: Van Nostrand–Reinhold)
[31] Ryan A T, Agrawal G P, Gray G R and Gage E C 1994 *IEEE Trans. Quantum Electron.* **30** 668
[32] Mørk J, Tromborg B, Mark J and Velichansky V 1992 *Proc. SPIE* **1837**
[33] Wieland J, Mirasso C R and Lenstra D 1997 *Opt. Lett.* **22** 469
[34] Sukow D W, Gardner J R and Gauthier D J 1997 *Phys. Rev.* A **56** R3370
[35] Kramers H A 1940 *Physica* **7** 284
[36] Kautz R L 1987 *Phys. Lett.* A **125** 315